

ON THE COMPOSITE NATURE OF THE GALAXY NGC 5929

GEORGI PETROV¹ & MICHEL DENNEFELD²

¹Institute of astronomy and National astronomical observatory, Sofia, Bulgaria

e-mail: petrov@astro.bas.bg

²Institut d'Astrophysique de Paris, University of Paris 6, Bd Arago FR 75014, Paris, France.

e-mail: dennefel@iap.fr

Abstract. The galaxy NGC 5929 is a member of the double system NGC 5929/5930. The two objects are at a distance of 0'.5 from each other. They figure under No. 90 in the Arp Catalogue of Peculiar Galaxies, and Zwicky mentioned them as compact objects (I Zw 112). Karachentsev included them under No. 466 in his catalogue of isolated double galaxies. Huchra et al. (1982) classified it as SyG type2. CCD spectra of the nucleus of the galaxy NGC 5929 for two different emission line regions obtained January 2012 with 1.93-m OHP telescope (M.D.) and covered spectral interval from $\lambda 3650$ to $\lambda 7300$ Å are analyzed. Dual emission line regions, reported from other authors too, are revised. A lot of emission lines as H α , H β , H γ , $\lambda 6300$, $\lambda 6363$ [OI], $\lambda 3727$ [OII], $\lambda 4959$, $\lambda 5007$ [OIII], $\lambda 6717$, $\lambda 6731$ [S II], $\lambda 6548$, $\lambda 6584$ [N H], $\lambda 6312$ [SIII], etc. and several absorption lines have been identified. The $\lambda 5199$ [N I] line is faintly visible, as well as the Fraunhofer absorption feature *b*, representing the neutral magnesium line $\lambda 5175$ Mg I. The components found in the line profiles of the NGC 5929 nucleus by other authors too can be interpreted as evidence for radial motion of gaseous masses at speeds of 200-300 km/sec. The physical parameters of the nucleus are estimated. The relative abundance of several ions is evaluated. For the emission-line spectrum to result from shock heating of the gas is inconsistent with the observational evidence. The discovery of kinematic shock signatures associated with a localized radio jet interaction in the merging Seyfert galaxy NGC 5929 and their interpretation the relative prominence of shocks to the high density of gas in nuclear environment as other models are briefly discussed.

1. INTRODUCTION

The galaxy NGC 5929 is a member of the double system NGC 5929/5930. The two objects are at a distance of 0'.5 from each other. They figure under No. 90 in the Arp Catalogue of Peculiar Galaxies (see Fig. 1a below), and Zwicky mentioned them as compact objects (I Zw 112). Karachentsev included them under No. 466 in his catalogue of isolated double galaxies. Huchra et al. (1982) classified it as SyG type2. NGC 5929 is nearby Seyfert galaxy. Because of its interesting optical and radio structure, it is investigated

very intensively – more then 300 references in SIMBAD and more than 270 in NED databases. During the last years the IR and X_ray investigations of NGC 5929 become leading.

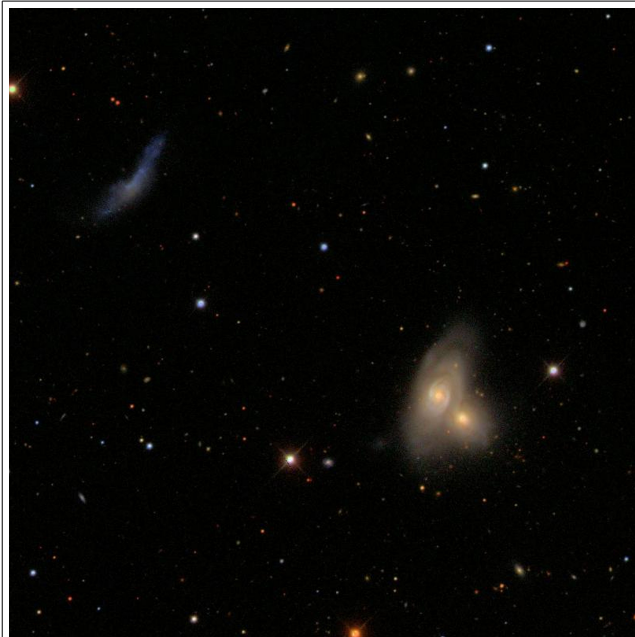


Figure 1a: SDSS Arp 90 = NGC5929/5930

CROSS-IDENTIFICATIONS for NGC 5929 ([Back to INDEX](#))

Object Names	Type	Object Names	Type
NGC 5929	G	USGC U703 NED04	G
UGC 09851	G	HOLM 710B	G
ARP 090 NED01	G	NPM1G +41.0399	G
VV 823 NED01	G	PGC 055076	G
I Zw 112 NED01	G	UZC J152606.1+414013	G
CGCG 222-007 NED01	G	FIRST J152606.1+414014	RadioS
CGCG 1524.3+4151 NED01	G	IRXP J152607.0+414016	XrayS
MCG +07-32-006	G	[SP82] 45	G
SDSS J152606.15+414014.3	G	LGG 399-[G93] 004	G
SDSS J152606.16+414014.4	G	[M98] 242 NED01	G
CG 0710	G	[VCV2001] J152606.1+414015	G
KPG 466 NED01	G	[RRP2006] 37	G
KPG 466A	G	[VCV2006] J152606.1+414015	G

Figure 1b: NGC 5929 – cross identifications

Figure 1b from NED shows all the crossidentifications of NGC 5929. In the Fig.2 below the integrated spectrum of NGC 5929 from SDSS is shown. A lot of absorption features and emission lines are identified.

N5929-SDSS RA=231.52566, DEC=41.67066, MJD=53149, Plate=1679, Fiber=350

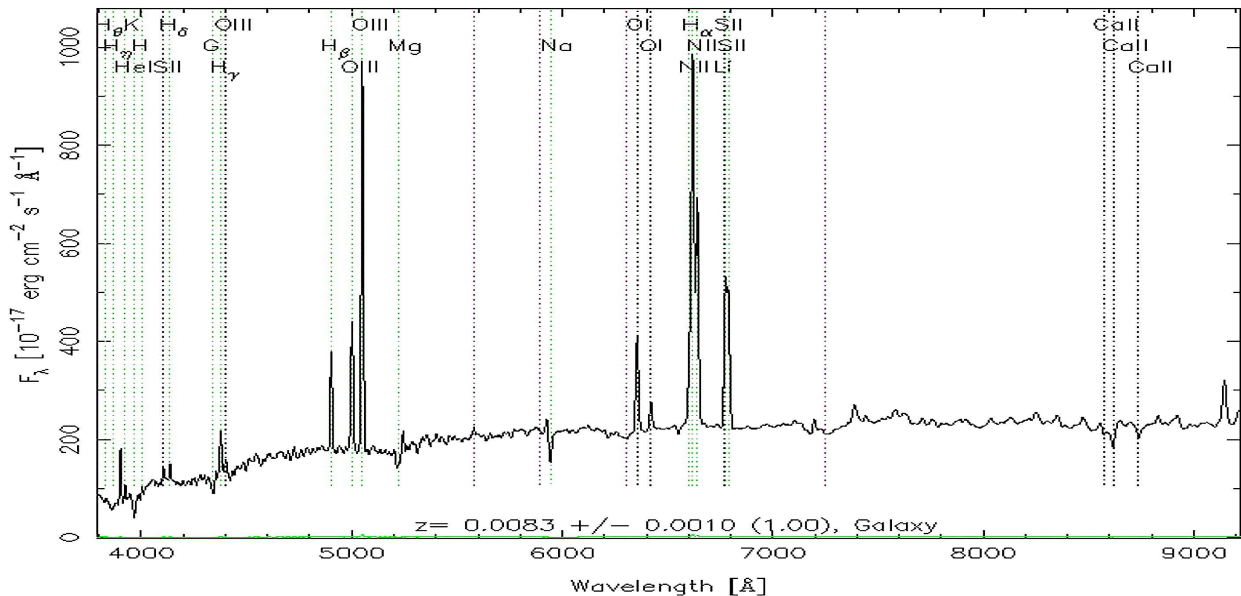


Figure 2: SDSS spectrum of NGC 5929

2. HISTORICAL OVERVIEW

Below we will try to have a look mainly of optical investigations of NGC 5929. First time double pick emission was shown in G. Petrov's PhD thesis (fig.12) using spectrograms obtained with the 125-cm reflector of the Crimean station, Shternberg Astronomical Institute. In the Fig.3 below the registrogram of the H_α regions of the spectrum of NGC 5929 is shown. Double_picked emission in the lines of [OI], [NII] and [SII] is clearly visible.

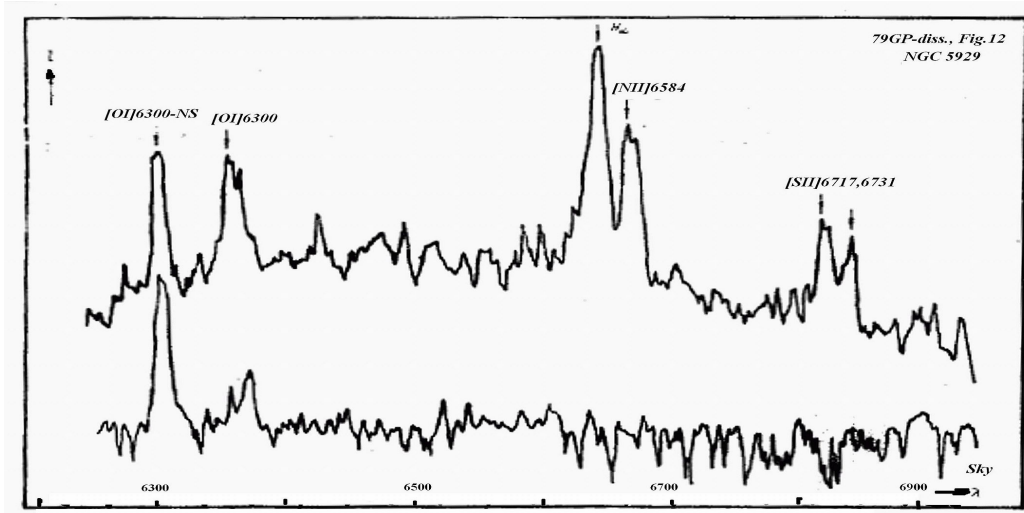


Figure 3: Registrograms of the spectra of NGC 5929 from the 6_m telescope.

The first spectrophotometric investigations of the integrated spectrum of the galaxy are presented in Petrov (1979a). Here NGC 5929 was classified as “emission-line galaxy”, not as a SyG one and double_pick emission is not commented. Spectra of the nucleus of the galaxy NGC 5929 obtained with the 1.25-m and 6-m telescopes show emission lines with separate components in the wings. In the blue and red wings of each line one can see components shifted 5-6 Å away from the center, nucleus appears to be devoid of structure. A spectrum of the other member of the pair, NGC 5930, obtained at the same resolution in wavelength, does not show components in the wings of the lines. The components we have found in the line profiles of the NGC 5929 nucleus can be interpreted as evidence for radial motion of gaseous masses at speeds of 200-300 km/sec (Golev et al. 1980). We make an evaluation the Ly_c-radiation of ca. 1000 young hot stars O5 V class in the nucleus of the galaxy is the most probable source of gas ionization.

Huchra et al. (1982) classified NGC 5929 as SyG type 2. Kennikutt & Keel (1984) investigated the effect of close galaxy-galaxy interactions on the level of nuclear activity in spiral galaxies. The demonstrates that “...galaxies with nearby companions possess significantly higher nuclear emission-line luminosities and equivalent widths, and their nuclei exhibit a significantly higher level of ionization on average. A much higher fraction of galaxies with Seyfert or Seyfert- type nuclei is found in the sample of multiple systems... The radio and optical results make a strong case for the presence of environmentally influenced nuclear activity in a significant fraction of spiral galaxies... In any case, it is clear that conditions in the nuclei are not isolated from the outer disks”. A low-dispersion spectrum taken through a 4.7-arcsec circular aperture shows a red continuum with absorption lines characteristic of an old population.

Keel (1985) investigates the “dual emission-line regions in the Seyfert galaxy NGC 5929”. He shows that the type 2 Seyfert nucleus of NGC5929 contains two emission regions situated symmetrically about the center of the galaxy with the ionization levels normally associated with Seyfert nuclei. Whittle et al. (1986) provided a detailed investigations of extended forbidden O III emission associated with nuclear radio lobes of the galaxy. As they mentioned, “...NGC 5929 is a nearby Seyfert 2 galaxy with particularly simple double-lobed radio structure. The [OIII] emission-line distribution closely matches that of the radio emission, showing two distinct components of different velocity straddling the optical nucleus. The Narrow

Line Region (NLR) of Seyfert galaxies appears to be closely related to the nuclear non-thermal radio emission...The absence of a young stellar population is evident from the 5150 Å continuum image, which shows no enhancement in the vicinity of the radio lobes”.

It is very likely Wakamatsu & Nishida (1988) to be the first authors showing the dual emission-line clouds take the place in the two member of the interacting pair Arp 90. “On optical spectra, dual-peak emission-line clouds have been discovered in both nuclei of an interacting pair Arp 90 (NGC 5929 + NGC 5930). The clouds in each galaxy are quite similar in their spatial, kinematical, and radio properties, but quite different in the excitation levels of the ionized gas, i.e., classified as H II region type for NGC 5930 or Seyfert 2 type for NGC 5929. NGC 5930 was detected as an IRAS source with the luminosity $L_{\text{IR}} = 2.0 \times 10^{10} L_{\text{sun}}$, while NGC 5929 was not...”. The authors have detected 2.6 mm CO (J = 1-0) line emission from the nuclear region of NGC 5930 but not from NGC 5929.

Taylor et al. (1989) explained the narrow emission lines of NGC 5929 with a plasmon driven bowshock model, in which the linear motion of radio-emitting bubbles of plasma ejected from the nucleus drives bowshocks into the ambient nuclear medium. The cooled shocked gas, photo-ionized by the UV nuclear continuum, produces the optical NLR emission. The two nuclear components at both radio and optical wavelengths of NGC 5929 galaxy they model as two plasmon driven bowshocks on either side of the nucleus.

In their “High-Resolution Observations Of The Multicomponent Nucleus of NGC 5929” Wilson & Keel (1989) shows “...the central region of the Type 2 Seyfert galaxy NGC 5929 is known to contain double radio-continuum and optical emission-line clouds separated by $\sim 1''$. When the radio continuum and [O III] 5007 image of Whittle et al. (1986) are compared at the same spatial resolution, there is no evidence that the separations or position angles of the radio and emission-line clouds differ. The double H $_{\alpha}$ clouds appear to differ in position angle by $\sim 20^{\circ}$ from the radio lobes..”.

Afanas'ev & Sil'chenko (1991) shows the two gas clouds being the main forbidden line emitters in the center of NGC 5929 are found to possess the relative line-of-sight velocities -50 km/s (the eastern cloud) and +270 km/s (the western cloud). They suppose “the emission brightness centers which coincide with the radio lobes are probably the shock wave regions forming on the border between the clouds and the galactic disk”.

HST Images of NGC 5929 and 5930 shows the nuclei of both galaxies contain emission line gas. Previous ground-based observations of the Seyfert galaxy NGC 5929 include [O III] and H $_{\alpha}$ + [N II] images, showing that its nucleus contains an elongated region of high-excitation emission line gas. In these HST images, this gas is clearly separated into two distinct regions separated by about $1''$... (Bower et al., 1993). Bower et al. (1994) shows the correspondence between the emission line gas and the radio morphology suggests that the structure of the NLR in NGC 5929 is governed by matter ejected from the AGN. The high-excitation gas in the narrow line region (NLR) of NGC 5929 is resolved into individual clouds in the central $1.5''$. Although the [O III] emission is clearly not spherically symmetric with respect to the nucleus and no direct evidence for the reddening and/or obscuration effects characteristic of a dusty torus, which, in the context of "unified models", is expected to obscure the active galactic nucleus (AGN) in type 2 Seyfert galaxies.

Su et al. (1996) confirm the triple radio structure reported in earlier studies. The weak central source of the triplet is almost certainly associated with the active nucleus... The radio structure of NGC 5929 to recent HST images was compared and the possible models to relate the radio and optical structures (bowshock model - Taylor et al. 1989), plasmon model (Pedlar et al. 1985) have been discussed.

Ferruit et al. (1997) report observations of the galaxy NGC 5929 with the integral field spectrograph Tiger covering the [NII], H $_{\alpha}$ and [SII] emission associated with the two radio-lobes. The two optical line emission components have been kinematically separated using Gaussian fitting of the spectra... All models predict edge-brightened bow shock or cylindrical shell structures for the ionized gas, which seems to conflict with the HST imaging. They noted the high spatial resolution spectrography is needed to obtain the

velocity structure of both the NE and SW components and to understand the relationship between the relativistic and thermal gases.

H II region population in a sample of nearby galaxies with nuclear activity have been studied by Gonzalez Delgado et al. (1997). They showed the emission-line morphology in the two disks of the interacting pair NGC 5929/C 5930 formed by a Sy2 nucleus, NGC 5929, and a starburst nucleus in a Sb galaxy, NGC 5930 are very different. NGC 5929 only shows some weak H II regions, however, the disk of NGC 5930 shows bright H II regions, mainly along the spiral arms.

Kotilainen (1998) detects extended blue continuum components in the circumnuclear region of several galaxies. These components form a double structure across the NGC 5929 nucleus. "...The nucleus of NGC 5929 is situated between two blue maxima at opposite sides of the nucleus... they possibly represent extranuclear scattering mirrors of anisotropically escaping nuclear light".

Ferruit et al. (1999) carry out spectroscopy of spatially resolved narrow line regions in NGC 5929 with HST Faint Object Spectrograph. It displays an "extended emission-line region with two main components, one blueshifted and one redshifted, located northeast and southwest of the nucleus, respectively. Radio observations show a triple radio source with two lobes straddling an unresolved nuclear component. Comparison between the radio maps and the emission-line observations reveals a close morphological and kinematical association between the ionized gas and the radio-emitting material. The observed line ratios are compared with the predictions of the two component (matter- and ionization-bounded, MB-IB), central source photoionization models of Binette et al. (1996) and of the fast, photoionizing ("autoionizing") shock models of Dopita & Sutherland (1995). In NGC 5929, the MB-IB models have problems reproducing the strengths of the neon lines, while shock/precursor models with a velocity ca. 300 km/s provide a good match to the data".

2000, Rhee & Larkin (2000) shows significant obscuration to the narrow-line region of the galaxy.

Gonzalez Delgado et al. (2001) search for the direct spectroscopic signature of massive stars and thereby probe the role of circumnuclear starbursts in the Seyfert phenomenon. They consider the possibility that there may be two distinct subclasses of Seyfert 2 nuclei - "starbursts" and "hidden broadline regions". NGC 5929 belongs to the group of objects with a continuum dominated by an old stellar population (the stellar lines are similar to those of an old population. Later-on Rainmann et al. (2003) showed the NGC 5929 galaxy is in a group dominated by 10-Gyr metal-rich stellar population (with solar or above metallicity).

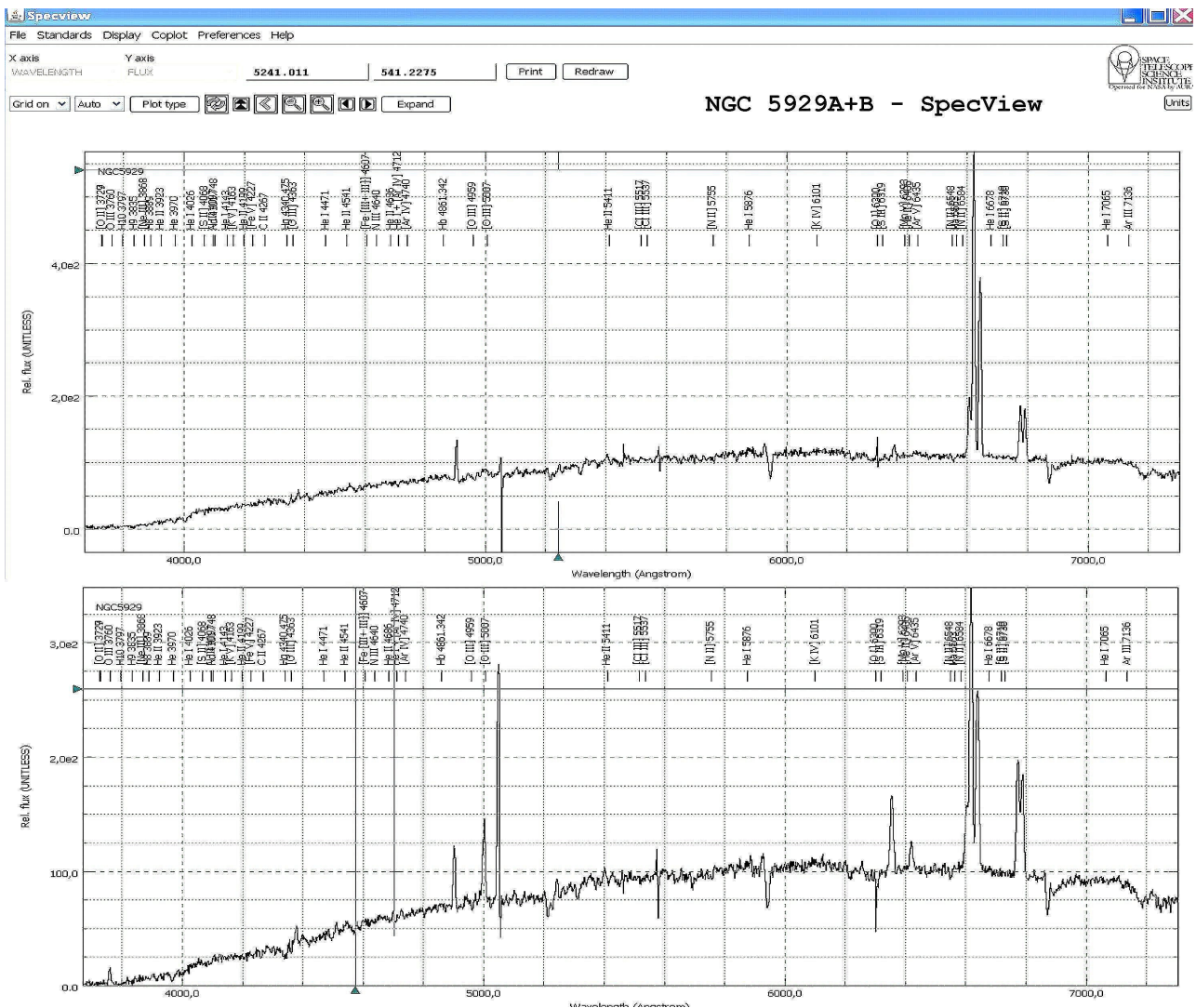
Rosario et al. (2010) carried out a direct detection of shocked gas studying the radio jet interaction in NGC 5929. They report the discovery of kinematic shock signatures associated with a localized radio jet interaction and find that low ionization gas at the interaction site is significantly more disturbed than high ionization gas, which we attribute to a local enhancement of shock ionization due to the influence of the jet. The characteristic width of the broad low-ionization emission is consistent with shock velocities predicted from the ionization conditions of the gas.

3. OBSERVATION AND REDUCTION

Spectra of the two emission-line regions of the galaxy NGC 5929 have been taken by prof. M. Dennefeld with the Carelec spectrograph attached to the 1.93 m OHP telescope during the night of 19/20/01/2012. The slit width was 2 arcsec. The spectra were reduced and calibrated by standard OHP MIDAS procedure. Table 1 below summarize the data for the telescope, spectrograph, CCD receiver, exposure time etc. Observed line fluxes are calibrated in 10^{-14} ergs s^{-1} cm^{-2} . Figure 4 below shows the two spectra – of NE and SW lobes of NGC 5929, using SPECVIEW possibilities to add some typical emission nebulae lines.

Table 1: Observational data for our spectrophotometric study of NGC 5929

Date of observation:	19.01.2012 r.
Telescope and spectrograph:	1.93_m OHP telescope, CARELEC spectrograph
Spectroscopic data:	136 A/mm, $\lambda\lambda$ 3600 – 7200 A,
	slit: width = 0.302 mm – corresponding to 2 arcsec on the sky
	length = 50 mm - corresponding to 5.5 arcmin on the sky
Observer:	prof. M. Dennefeld
Time exposure:	1800 sec
Dev_type:	CCD EEV 42-20
Objects:	NGC 5929A = NE_lobe, NGC 5929B = SW lobe of NGC 5929
Observed line flux:	in 10^{-14} ergs s^{-1} cm^{-2}



The two calibrated spectra are finally reduced in the same manner to get all the spectrophotometric data using ESO MIDAS package (Grosbol & Ponz 1990). The line fluxes were determined using the two possibilities of MIDAS – context LONG and context ALICE. Figure 5 below demonstrates INTEGRATE/LINE procedure of the context LONG. The spectra were subdivided in 3 parts covering ca. 1000 Å. The continuum was interactively determined by the two points from the both sides of each line – absorption or/and emission.

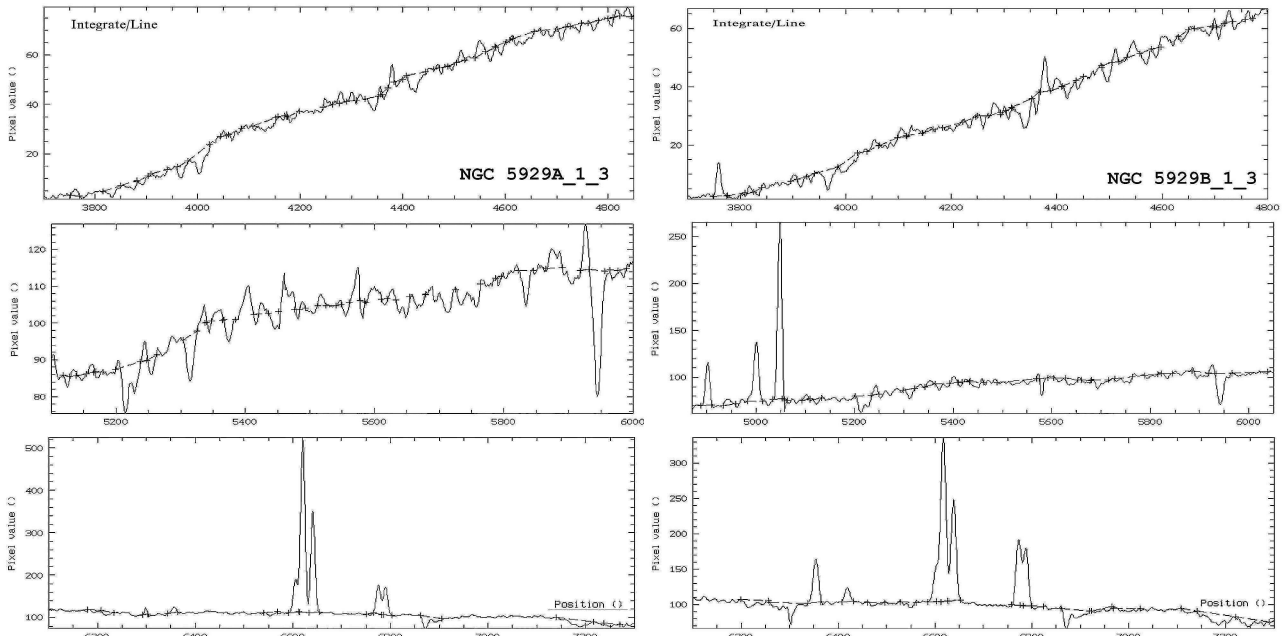


Figure 5: Results from MIDAS “INTEGRATE/LINE” procedure for NGC 5929A and B.

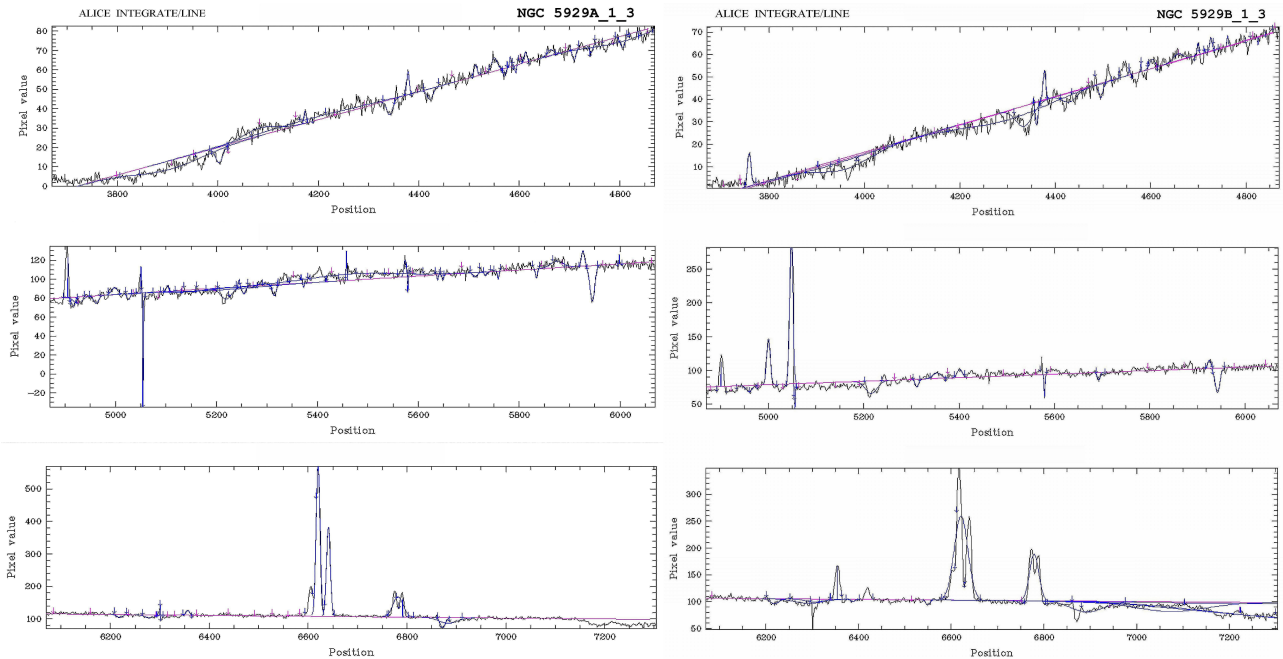


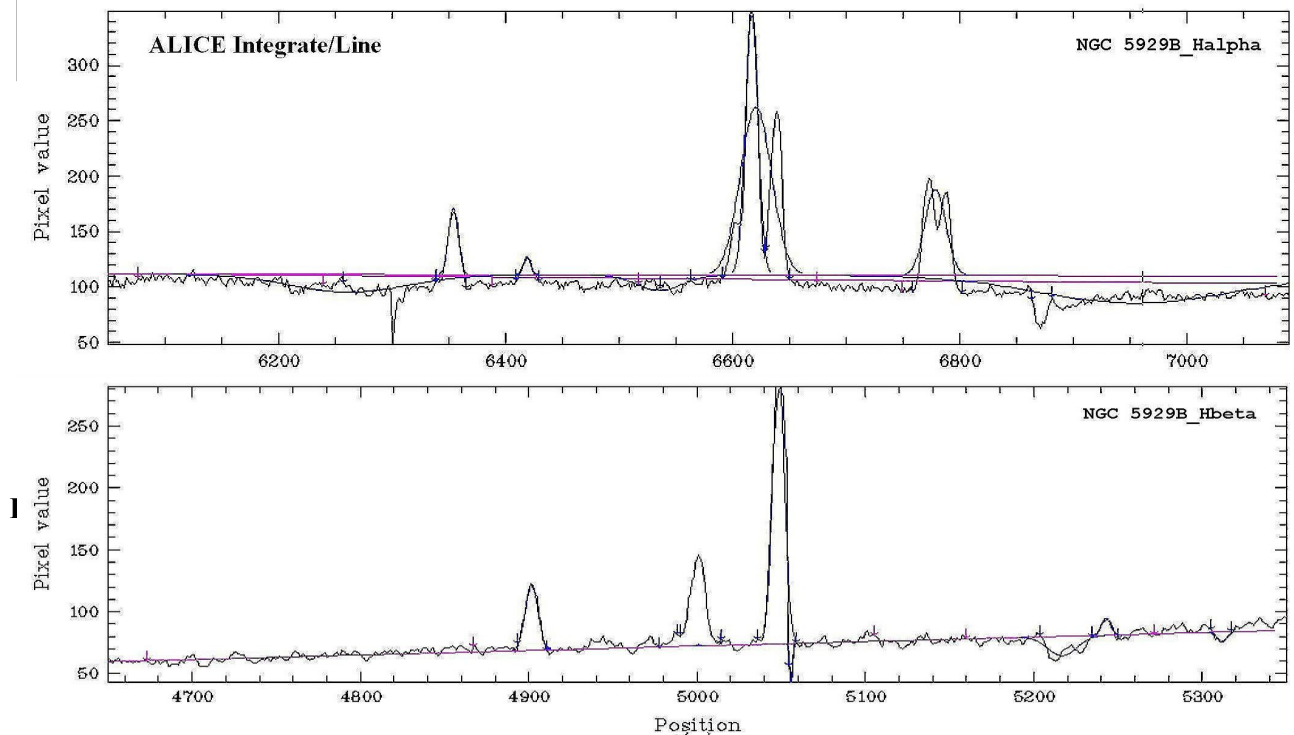
Figure 6: Results from MIDAS “ALICE - INTEGRATE/LINE” procedure for NGC 5929A and B.

Figure 6 demonstrates ALICE INTEGRATE/LINE procedure. The same spectra subdivided in 3 parts covering ca. 1000 Å each were used. The continuum showed by continuous line was determined by ca. 20 points over the spectra fitted by different order polynoms.

Table 2 summarize the results of emission and absorption lines identifications, equivalent widths and fluxes for NE (NGC 5929A) and SW (NGC5929B) lobes of the galaxy. Absorption features bandpasses are mainly acc. to Trager et al. (1998).

Table 2: n5929A&B – fluxes and EQWT			Rem: EQWT<0 means emission			
Objects			NGC 5929A		NGC5929B	
X0	Ident	Bandpass	Flux	EQWT	Flux	EQWT
3727.42	[OII]		21.05	-6.26	106.33	-38.02
3840.00	H9_blend	3822-3858	-25.09	3.35		
3868.76	[NeIII]				18.47	-2.43
3889.00	HeI&H8				-25.70	2.94
3930.00	K_CaII	3908-3952	-65.78	4.15	-67.71	6.50
3970.00	H_CaII	3952-3988	-160.59	7.78	-55.17	3.91
4068.60	[SII]				28.52	-1.25
4225.44	Ca4227	4222-4234			-25.89	0.86
4301.00	G_band	4284-4318	-72.48	1.70	-177.25	5.15
4340.48	H_gamma		61.05	-1.29	109.85	-2.86
4368.74	[OIII]+?	Blend?			37.76	-0.96
4386.06	Fe4383	4369-4420	-147.29	2.81	-48.37	1.18
4471.60	HeI		26.24	-0.45	23.78	-0.49
4536.88	Fe4531	4514-4559	-42.52	0.68	-49.10	1.29
4541.60	HeII		7.19	-0.12		
4552.00	Fe4531	4514-4559	-38.54	0.60		
4656.25	C2-4668	4634-4720	-40.84	1.24		
4668.62	C2-4668	4634-4720			-43.48	0.70
4685.70	HeII		22.69	-0.32	25.24	-0.41
4698.23	C2-4668	4634-4720	-32.30	0.45		
4861.34	H_beta		403.47	-5.28	456.73	-6.50
4871.98	Hbeta	4847-4876	-27.66	0.36		
4893.40	[FeVII]				65.58	-0.92
4924.00	FeII				-37.29	0.51
4931.00	[OIII]		34.45	-0.43	12.64	-0.17
4958.90	[OIII]				753.70	-10.09
4972.10	[FeVI]		14.47	-0.18		
5006.80	[OIII]				1820.00	-23.50
5015.55	Fe5015	4977-5054	-245.40	2.96		

5027.85	Fe5015	4977-5054			-28.75	0.76
5102.90	Mg1	5069-5134			-57.63	1.07
5107.89	Mg1	5069-5134	-7.30	0.36		
5158.98	[FeVII]		15.80	-0.18		
5168.29	Mg2	5154-5196	-198.57	2.25	-306.15	3.85
5191.82	[ArIII]		78.06	-0.96		
5199.00	[NI]		30.17	-0.34	78.06	-0.96
5270.20	Fe5270	5245-5285	-144.90	1.50	-126.41	1.42
5328.43	Fe5335	5312-5352	-48.00	0.48	-93.23	1.00
5398.30	Fe5406	5387-5415	-86.55	0.83		
5423.90	[FeVI]		29.26	-0.28		
5517.66	[CIII]		68.35	-0.65	27.19	-0.28
5630.82	[FeVI]		19.44	-0.18		
5699.24	Fe5709	5696-5720	-102.62	0.94	-112.99	1.13
5784.96	Fe5782	5776-5796	-102.07	0.89	-45.76	0.44
5790.70	Hg		-87.50	0.77	-46.96	0.45
5875.65	HeI		114.32	-1.01	65.61	-0.63
5897.23	NaD	5876-5909	-411.68	3.80	-471.42	4.54
5971.30	TiO1	5936-5994	-22.87	0.20	-107.41	1.02
6228.50	TiO2	6189-6272	-124.97	1.14	-591.21	5.79
6300.00	[OI]		145.08	-1.32	783.29	-7.62
6363.80	[OI]+?				239.90	-2.31
6374.00	[FeX]				227.61	-2.18
6548.88	[NII]		766.65	-7.00	754.41	-7.20
6562.81	H_alpha		4387.74	-38.96	3308.84	-31.70
6583.83	[NII]		2494.67	-22.30	1928.58	-18.24



X_start	X_end	Flux	EQWT	X0	Ident
4953.74	4970.56	-39.76	0.50	4920.510	Fe I
4983.88	5010.51	134.27	-1.63	4958.930	[O III]
5039.95	5051.16	73.19	-0.87	5006.860	[O III]
5051.16	5068.68	-273.54	3.27	5015.000	
5239.00	5248.11	36.12	-0.40	5197.940	[N I]
5239.00	5248.11	36.12	-0.40	5200.410	[N I]
5302.08	5326.61	-156.76	1.62	5269.550	Fe I
6590.32	6612.28	942.80	-8.49	6548.060	[N II]
6606.59	6630.99	4741.59	-42.39	6562.808	H_alpha
6630.99	6654.58	2580.90	-23.23	6583.370	[N II]
6763.60	6784.75	771.67	-6.99	6716.420	[S II]
6781.49	6800.20	731.93	-6.87	6730.780	[S II]

4. SPECTROPHOTOMETRIC STUDY

Table 4 presents all the spectrophotometric results for the two emission regions. Identifications, equivalent widths, fluxes and flux ratios are summarized. The highest ionization stage line in NGC 5929A is $\lambda 5159$ [FeVII] and in NGC 5929B – $\lambda 6374$ [FeX]. Forbidden lines of N° doublet [NI] $\lambda 5199$, C⁺⁺ - [CIII] $\lambda 5517$, HeI $\lambda\lambda 4472, 5876$ and HeII $\lambda\lambda 4686, 5411$ present in both spectra. Unexpected is a present of serial of [FeVI] lines in NGC 5929A and a present of less prominent [OIII] line $\lambda 4931$ when the “traditional” $\lambda\lambda 4959, 5007$ are missing (see below). Low ionization forbidden lines of [OI] $\lambda 6300$, [OII] $\lambda 3727$, [NII] $\lambda\lambda 6548, 6584$ and [SII] $\lambda\lambda 6717, 6731$ present in both spectra too. H α /H β flux ratio – 10.845 for NGC 5929A and 7.245 for NGC 5929B confirms significant obscuration to the narrow-line region of the galaxy, mentioned by Rhee & Larkin (2000).

Object			NGC 5929A			NGC 5929B		
Seq	X0	Ident	Flux	EQWT	F/F_H β	Flux	EQWT	F/F_H β
1	3727.42	[OII]	21.05	-6.26	0.052	106.33	-38.02	0.233
2	3868.76	[NeIII]				18.47	-2.43	0.040
3	4068.60	[SII]				28.52	-1.25	0.062
4	4340.48	H_gamma	61.05	-1.29	0.15	109.85	-2.86	0.240
5	4368.74	[OIII]+?				37.76	-0.96	0.083
6	4471.60	HeI	26.24	-0.45	0.065	23.78	-0.49	0.052
7	4541.60	HeII	7.19	-0.12	0.018			
8	4685.70	HeII	22.69	-0.32	0.056	25.24	-0.41	0.055
9	4861.34	H_beta	403.47	-5.28	1.00	456.73	-6.50	1.00
10	4893.40	[FeVII]				65.58	-0.92	0.144
11	4931.00	[OIII]	34.45	-0.43	0.085	12.64	-0.17	0.028
12	4958.90	[OIII]				753.70	-10.09	1.650

13	4972.10	[FeVI]	14.47	-0.18	0.036			
14	5006.80	[OIII]				1820.00	-23.50	3.985
15	5158.98	[FeVII]	15.80	-0.18	0.039			
16	5199.00	[NI]	35.28	-0.39	0.087	78.06	-0.96	0.171
17	5410.80	HeII	56.16	-0.54	0.139	27.19	-0.28	0.060
18	5423.90	[FeVI]	29.26	-0.28	0.072			
19	5517.66	[CIII]	68.35	-0.65	0.169	65.61	-0.63	0.144
20	5630.82	[FeVI]	19.44	-0.18	0.048	783.29	-7.62	1.715
21	5875.65	HeI	114.32	-1.01	0.283	239.90	-2.31	0.525
22	6300.00	[OI]	145.08	-1.32	0.360	227.61	-2.18	0.498
23	6363.80	[OI]+?				1134.14	-10.96	2.483
24	6374.00	[FeX]				227.61	-2.18	0.498
25	6548.88	[NII]	1099.54	-9.83	2.725	754.41	-7.20	1.652
26	6562.81	H_alpha	4387.74	-38.96	10.875	3308.84	-31.70	7.245
27	6583.83	[NII]	2494.67	-22.30 6	183	1928.58	-18.24	4.222
28	6716.42	[SII]	807.25	-7.42	2.001	1286.89	-13.01	2.818
29	6730.78	[SII]	730.68	-6.91	1.811	1290.31	-13.10	2.825

In Tabl.5 we summarize some important flux ratios to check the validity of some models above mentioned by Ferruit et al. (1999), using Binette et al. 1996 (B96) and Binette et al. 1997 (B97) models. In our opinion our observational data do not fit well with any of these models. Remember Ferruit et al (1999) observed with HST/FOR SW lobe only – i.e. “our” NGC 5929B and the two spectrophotometric serials are quite different – e.g. $H\alpha/H\beta = 4.7$ and 7.2 respectively. As their result differs from others observations too one possible explanation could be changes in the physical conditions and ionization status of the emitting gas. Electron temperature defined by [OIII] ratios is ca. 14000 K and the electron densities in the [SII] – [OII] zone are ca. $4 - 5 \cdot 10^2 \text{ cm}^{-3}$. Our previous spectrophotometric study based on the integrated spectra of NGC 5929 are presented in Petrov (1979b). In the same time [OIII] $\lambda 4931$ line tell us for electron densities of 40 cm^{-3} as the critical electron density for this line to be observable is 40 cm^{-3} (Gurzadyan 1997). These evaluations confirm models with quite complex cloud structure with different temperatures, densities and ionization stages.

	NGC 5929A	NGC 5929B	models	
Rad. Velocities [km/sec]	2595	2526	$V_s = 300 \text{ km/s}$ (B96)	L_model (B97)
Ratio				
[OIII] 5007 / Hbeta		3.956	5.9 – 6.5	0.32 – 0.58
[OII] 3727 / Hbeta	0.017	0.232	1.7 – 5.2	< 0.62
[OI] 6300 / Halpha	0.033	0.254	0.32 – 0.47	< 0.39
[OII] 3727 / [OIII] 5007		0.058	0.3 – 0.8	0.57 – 0.28
[OI] 6300 / [OIII] 5007		0.300	0.15 – 0.23	0.35 – 0.17

[OIII] 5007 / [OIII] 4363		48.20	103 - 108	3.8 – 0.78
[NII] 6583 / Halpha	0.568	0.590	0.23 – 0.65	< 101
[SII] 6724 / Halpha	0.350	0.785	0.41 – 0.56	2.3 – 0.30
[He II 4686 / Hbeta	0.056	0.055	0.23 – 0.28	< 0.57
[NeIII] 3869 / Hbeta		0.040	0.50 – 0.72	1.0 – 8.7
[SII] 6717 / [SII] 6731	1.105	1.129		
[OIII] 4959+5007 / [OIII] 4363		68.16		
Ne for Te = 10 000 K	470	450		

Table 6: Abundances of some ions for Te = 10 000K;		Log H = 12.00	
		NGC 5929A	NGC 5929B
Log N+ (λ 6584/Hbeta)		7.99	7.83
Log S+ (λ (6717+6731)/Hbeta)		7.22	7.39
Log O++ (λ 5007/Hbeta)		-	8.10
Log O+ (λ 3727/Hbeta)		5.96	7.00
Log O° (λ 6300/Hbeta)		7.70	7.84
Log He+ (λ 5876/Hbeta)		11.32	11.59
Log He++ (λ 4685/Hbeta)		9.75	9.74

Based on the spectrophotometric data some evaluations of ionic abundances have been made using the methods of Pagel et al. (1979), Peimbert (1968, 1995), Oey & Shields (2000) etc. No total elemental abundances have been determined because of the lack of near IR spectra or low spectral resolution. In Tabl.6 abundances of some ions are presented assuming electron temperature $T_e = 10000$ K. As usual hydrogen abundance was set to $\text{Log}H = 12.00$. These results are close to our previous determination of the ionic abundance from the integrated spectrum of NGC 5929. In the Tabl.7 below we summarize average ionic N+ and S+ abundances for different kind of emission type objects – from PIN and HII regions to SyG. Pay attention – these are ionic abundances and not a chemical composition – i.e here we include ionization stage of the emitting regions.

Table 7: Average ionic N+ and S+ abundances for some kinds of emission type of objects.														
	PIN		HII regions		Mrk Gal		Akn Gal		SyG type 2		SyG type1		Norm.Gal	
	LgN+	LgS+	LgN+	LgS+	LgN+	LgS+	LgN+	LgS+	LgN+	LgS+	LgN+	LgS+	LgN+	LgS+
<X>	6.58	5.37	6.91	6.11	7.34	6.68	7.43	6.82	7.54	6.70	6.27	5.51	7.71	6.76
σ	0.84	0.63	0.41	0.32	0.22	0.30	0.20	0.36	0.26	0.29	0.44	0.44	0.34	0.26
n	37	28	36	37	28	23	18	14	28	28	25	23	20	17

Detailed results from the spectrophotometric investigation and chemical abundance of the two lobes of the galaxy together with some modeling of the cloud structure will be an object of another paper.

5. CONCLUSION

Based on the low resolution spectra from the 1.93 m OHP France telescope and CARELEC spectrograph we provided a preliminary study of the two emission lobes of the Seyfert galaxy NGC 5929. A lot of absorption features and emission lines have been identified in the two lobes. Evidences for low density clouds with $N_e \sim 40 \text{ cm}^{-3}$ in the two lobes are presented, based on the presence of [OIII] $\lambda 4931$ line.

NGC 5929A (i.e. NE-lobe) is an old star dominated region with a lot of absorption features. No signs of young stellar population have been found in accordance with the previous investigations. [OII]-[NII]-[SII] zone is characterized with $N_e \sim 470 \text{ cm}^{-3}$. No independent determination of the electron temperature was possible. Ionic abundances is quite higher in comparison with different type of emission line objects. The highest ionization lines are [FeVII] $\lambda 5159 \text{ \AA}$. It is remarkable to mention absence of [OIII] $\lambda \lambda 4363, 4959$ and 5007 \AA . Redshift determined from the emission line spectrum is $z = 0.00865$.

NGC 5929B (i.e. SW-lobe) is a typical Sy2G spectrum with a lot of strong emission lines. Redshift determined from the emission line spectrum is $z = 0.00842$. The highest ionization lines are [FeX] $\lambda 6374 \text{ \AA}$. Electron temperature in the [OIII] zone is ca. 14000K and the electron density in [OII]-[NII]-[SII] zone is characterized with $N_e \sim 450 \text{ cm}^{-3}$. Ionic abundances is quite higher in comparison with different type of emission line objects. N^+ ionic abundances ($\lg N^+ = 7.83$) is lower than in NGC 5929A ($\lg N^+ = 7.99$) but all other ionic abundances are higher – e.g. $\lg O^+ = 5.96$ and 7.00 respectively. Remember practically no O^+ in NGC 5929A.

References

- Afanas'ev, V. L., Sil'chenko, O. K.: 1991, *BSAO*, **33**, 103.
- Binette, L., Wilson, A. S., Raga, A., Storchi-Bergmann, T.: 1997, *A&Ap*, **327**, 909.
- Binette, L., Wilson, A. S., Storchi-Bergmann, T.: 1996, *A&Ap*, **312**, 365.
- Bower, G. A., Wilson, A. S., Mulchaey, J. S., Miley, G. K., Heckman, T. M., Krolik, J. H.: 1993, *BASS*, **182**, 406.
- Bower, G. A., Wilson, A. S., Mulchaey, J. S., Miley, G. K., Heckman, T. M., Krolik, J. H.: 1994, *AJ*, **107**, 1686.
- Dopita, M. A., Sutherland, R. S.: 1995, *ApJ*, **455**, 468.
- Ferruit, P., Pecontal, E., Wilson, A. S., Binette, L.: 1997, *A&Ap*, **328**, 493.
- Ferruit, P., Wilson, A. S., Whittle, M., Simpson, C., Mulchaey, J. S., Ferland, G. F.: 1999, *ApJ*, **523**, 147.
- Golev, V. K., Yankulova, I. M., Petrov, G. T.: 1980, *Sov.Astr.Lett.*, **6**, 290.
- Gonzalez Delgado, R. M., Heckman, T., Leitherer, C.: 2001, *ApJ*, **546**, 845.
- Gonzalez Delgado, R. M., Perez, E., Tadhunter, C., Vilchez, J. M., Rodriguez-Espinosa, J. M.: 1997, *ApJ Suppl.Ser.*, **108**, 155.
- Grosbøl, P.J., Ponz, J.D.: 1990, In: *Acquisition, Processing and Archiving of Astronomical Images*, p. 109. G. Longo and G. Sedmak (eds.), OAC and FORMEZ.
- Gurzadyan, G. A.: 1997, *The physics and dynamics of planetary nebulae*. Springer-Verlag Berlin Heidelberg.
- Huchra, J. P., Wyatt, W. F., Davis, M.: 1982, *ApJ*, **86**, 1628.
- Keel, W. C.: 1985, *Nature*, **318**, 43.
- Kennicutt, R. C., Jr., Keel, W. C.: 1984, *ApJ*, **279**, L5.
- Kotilainen, J. K.: 1998, *A&A Suppl.Ser.*, **132**, 197.
- Oey, M. S., Shields, J. C.: 2000, *ApJ*, **539**, 687.
- Pagel, B. E. J., Edmunds, M. G., Blackwell, D.E., Chun, M. S., Smith, G.: 1979, *MNRAS*, **189**, 95.
- Pedlar, A., Dyson, J. E., Unger, S. W.: 1985, *MNRAS*, **214**, 463.
- Peimbert, M.: 1968, *ApJ*, **154**, 33.
- Peimbert, M.: 1995, In: "The Analysis of Emission Lines", ed. R. E. Williams, Cambridge University Press.
- Petrov, G.: 1979a, *Sov.Astr.Lett.*, **5**, 141.
- Petrov, G.: 1979b, *Astrofizika*, **17**, 43.
- Raimann, D., Storchi-Bergmann, T., Gonzalez Delgado, R. M., Fernandes, R. C., Heckman, T., Leitherer, C., Schmitt, H.: 2003, *MNRAS*, **339**, 772.

Rhee, J. H., Larkin, J. E.: 2000, *ApJ*, **538**, 98.
Rosario, D. J., Whittle, M., Nelson, C. H., Wilson, A. S.: 2010, *ApJ*, **711**, L94.
Su, B., M., Muxlow, T. W. B., Pedlar, A., Holloway, A. J., Steffen, W., Kukula, M. J., Mutel, R. L.: 1996, *MNRAS*, **279**, 1111.
Taylor, D., Dyson, J. E., Axon, D. J., Pedlar, A.: 1989, *MNRAS*, **240**, 487.
Trager, S. C., Worthey, G., Faber, S. M., Burstein, D., Gonzalez, J. J.: 1998, *ApJ Suppl.Ser.*, **116**, 1.
Wakamatsu, K.-I., Mitsugu T. Nishida, M. T.: 1988, *ApJ*, **325**, 596.
Whittle, M., Haniff, C. A., Ward, M. J., Meurs, E. J. A., Pedlar, A., Unger, S. W., Axon, D. J., Harrison, B. A.: 1986, *MNRAS*, **222**, 189.
Wilson, A. S., Keel, W. C.: 1989, *AJ*, **98**, 1581.